A Synoptic Climatology of Northwest-Flow Severe Weather Outbreaks. Part II: Meteorological Parameters and Synoptic Patterns

ROBERT H. JOHNS

National Severe Storms Forecast Center, Kansas City, MO 64106

(Manuscript received 4 February 1982, in final form 9 November 1983)

ABSTRACT

A climatology of meteorological parameters and synoptic patterns associated with severe weather outbreaks occurring in areas where the mid-tropospheric flow has a north of west component is presented. This climatology utilizes data and criteria previously described by Johns. A comparison of the northwest flow parameters and those associated with general severe weather is given. The importance of conditional instability and low-level warm advection in northwest flow situations is discussed. An explanation is offered for the location of the axes of highest frequency of northwest flow outbreaks. Furthermore, the varying nature of wind shear associated with severe weather is discussed and the importance of the directional contribution of wind shear to northwest flow severe weather is demonstrated.

1. Introduction

Severe weather forecasters have noticed that meteorological parameters and synoptic patterns associated with northwest flow (NWF) outbreaks often differ from those found in the typical southwest flow outbreak situations. Miller (1972) has outlined some general NWF synoptic patterns based mostly on subjective experiences. Several others have conducted regional studies in which NWF patterns and parameter values are identified (e.g., Galway, 1958; Notis and Stanford, 1973, 1976; David, 1977; Giordano and Fritsch, 1983). However, little has been done to examine objectively the NWF phenomenon over a large domain. Therefore, the comprehensive NWF data set described in Part I (Johns, 1982b) has been used to develop a climatology of the meteorological parameters and synoptic patterns associated with NWF outbreaks. Unique features of this climatology help to explain 1) the importance of low-level warm advection in NWF outbreak initiation, 2) the pattern of NWF frequency distribution, and 3) the role of synoptic-scale wind shear in severe local storm development.

2. Climatology of meteorological parameters

a. 500 mb parameters

Composite charts from regional studies (Galway, 1958; David, 1977) suggest that NWF severe weather usually occurs to the south (on the anticyclonic shear side) of the 500 mb jet. Examination of the NWF data set (Johns, 1982b) reveals that this is indeed a common characteristic of NWF outbreaks regardless of area of occurrence. Of the 163 NWF cases used in this study, almost nine-tenths (88%) occurred along and/or to the south of the 500 mb jet.

David's (1977) 500 mb composite chart for NWF tornadoes in New England shows most of the 500 mb cold advection and height falls to the north of the outbreak area, with little amplitude in the isotherms or height contours south of the jet axis. Inspection of the 500 mb charts in the NWF data set reveals that this characteristic is also common to NWF outbreaks in general. Thus, it is not surprising that there is usually little 500 mb temperature or height change over an outbreak area during the event.[1] In nearly two-thirds of the 163 cases, the temperature either did not change or actually increased. Similarly, in more than half the outbreaks, the height either remained the same or increased. In only about one-fourth of the cases did the height fall more than 10 m.

Miller (1972) has identified the strength of the middle level jet (approximately 3–6 km above sea level) as a valuable parameter in the production of severe weather. From this study it has been determined that over two-thirds of all NWF outbreaks are associated with 500 mb wind maxima of 26 m s^{-1} (50 kt) or greater.[2] Furthermore, for every month of the NWF season (May–August), the *average* 500 mb wind maximum

[1] Twelve-hour change from 5A chart to 5B chart. Chart 5A refers to the 500 mb chart based on observations taken at least 2 h before the beginning of the outbreak and chart 5B to the 500 mb chart for 12 h after chart 5A. (See Johns, 1982b.)

[2] 500 mb jet-wind maxima were determined for 161 of the NWF cases. In those cases where it was not clear which maximum was associated with the outbreak, the closest maximum was used. In two cases, no 500 mb jet was present within 1200 km of the outbreak area.

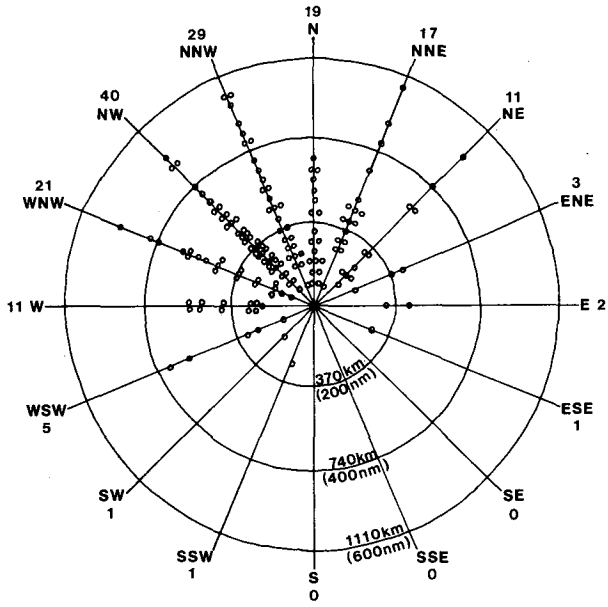

FIG. 1. Schematic diagram representing locations of 500 mb wind maxima relative to the geographical midpoints of 161 NWF outbreaks (1962–77). Number of maxima in the direction of each of the 16 compass points is indicated.

for outbreak events is greater than 26 m s^{-1}. The locations of the 500 mb jet maxima at the temporal midpoint[3] of each outbreak are shown in Fig. 1. The locations are relative to the geographical (spatial) midpoint of the outbreak. Note how most (78%) of the speed maxima are located from a west-northwesterly direction to a north-northeasterly direction from the outbreak centerpoint. The relative locations of the maxima vary little regionally (see Johns, 1982b) except in the Southern Plains, where almost half (46%) of the maxima occur in the northeast quadrant relative to the centerpoint. Almost three-quarters (74%) of the 500 mb wind maxima are located within 550 km (300 n mi) of the centerpoint, while only one-tenth (11%) occur at a distance greater than 750 km. There is little regional variation in the distances.

Most of the 500 mb parameters examined show little change from month to month during the primary NWF season. However, the monthly means for both temperature and height reach a peak in July, when the average temperature is −8.6°C and the average height is 5860 m.[4] A 500 mb temperature of −6°C appears to be a threshold temperature, since only two of the 163 outbreaks occurred with warmer 500 mb conditions. It may be that this 500 mb temperature is related to correspondingly warm conditions between 800 mb and 650 mb that act as a "cap" preventing vigorous convective development. Fig. 2 illustrates some of the regional differences in the 500 mb parameters associated with NWF outbreaks. The average 500 mb height in the Northeast region is significantly higher than the average height in the Upper Mississippi Valley region. This difference appears to be related to the fact that many Upper Mississippi Valley region outbreaks occur early in the NWF season, while almost all of the Northeast region cases occur in July and August (Johns, 1982b). Note the relatively low values for wind speed maxima in the Great Plains states. This anomaly is discussed in Section 4.

b. 850 mb parameters

Temperature and moisture values at 850 mb with NWF outbreaks are rather high compared with those associated with severe weather in general (David, 1976; Miller, 1972). Over 70% of all NWF outbreaks are associated with 850 mb temperatures of 20°C or greater and dewpoints of 12°C or more. These high NWF values are generally a reflection of the time of year of occurrence (late spring and summer). However, even during the months of peak NWF activity, data sources suggest that the 850 mb temperatures and dewpoints associated with NWF outbreaks have higher average values than those same parameters in general severe weather situations. For example, in July, mean 850 mb temperature and dewpoint values for NWF outbreaks are the highest for any month, averaging 22°C and 14°C respectively. In comparison, David (1976)

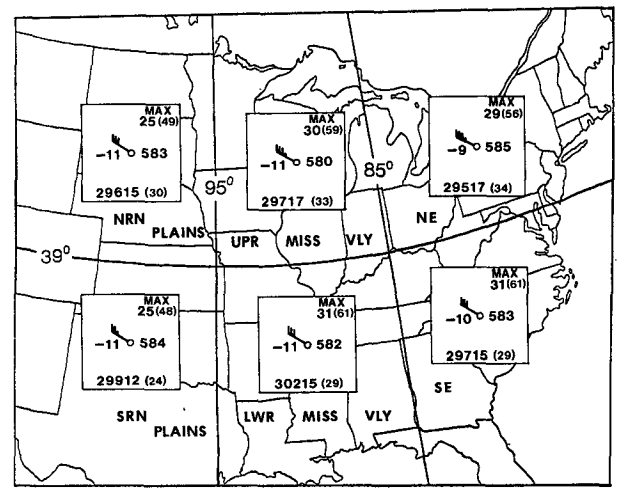

FIG. 2. Regional variations in the 500 mb parameters associated with NWF outbreaks. Relative to station circle, average temperature (°C) is to the left, average height (dam) is to the right, average wind direction and speed (m s^{-1} with knots in parentheses) is below, and average wind maximum (m s^{-1} with knots in parentheses) with associated short wave is to the upper right. Wind barb shows average wind direction and speed (full barb signifies 5 m s^{-1}).

[3] The temporal midpoint of an outbreak has been defined as that time midway between the first and last reports of severe weather. The location of the jet maximum at each midpoint time has been interpolated from 500 mb charts prepared from data obtained at the nearest standard radiosonde observation times on either side of the midpoint time.

[4] Values at the time of the 5A chart (See Johns, 1982b).

found that the *highest* monthly averages for all July tornado occurrences are only 19°C and 11°C for temperature and dewpoint, respectively. There are several possible explanations for these differences, some meteorological and some technical.[5] As a possible meteorological explanation, recall that Section 2a suggests that NWF outbreaks are generally confined to areas where the influence of 500 mb short-wave troughs is relatively weak. Therefore, other severe weather parameters must compensate for the weak dynamics. It appears that in most NWF situations a key factor is the high degree of conditional instability present (see Section 2c) resulting from high values in the low-level thermal and moisture fields. Maddox and Doswell (1982) have shown that significant severe weather episodes can occur under weak dynamic regimes when the air mass has a high degree of conditional instability and pronounced low level warm advection is present in the area. An examination of several of the NWF cases suggests that pronounced 850 mb warm advection is almost always present in the genesis area of NWF outbreaks.

Most (70%) of the 850 mb wind directions associated with NWF outbreaks are from the southwest quadrant (190–270°). However, over one-fifth (21%) of all NWF outbreaks occur with 850 mb winds from the northwest quadrant (280–360°). Northwesterly 850 mb wind cases are biased towards the peak of the NWF outbreak season, with well over half such cases occurring during the month of July. In fact, 40% of all NWF cases occurring in the month of July have 850 mb winds from the northwest quadrant.

A geographical breakdown of the average 850 mb parameters (Fig. 3) shows that the low-level wind flow associated with NWF outbreaks is southerly in the Plains states, but veers with increasing distance eastward. Observe that the average 850 mb wind direction associated with those outbreaks east of 85° longitude is from the northwest quadrant (280°). This is consistent with David's (1977) findings for 850 mb wind directions associated with New England NWF tornadoes. Note that the wind pattern of Fig. 3 resembles the mean flow pattern around the Bermuda high which usually extends westward into the Gulf states during the summer season. The circulation around the high results in southerly low-level flow along the western periphery of the ridge and westerly flow to the north.

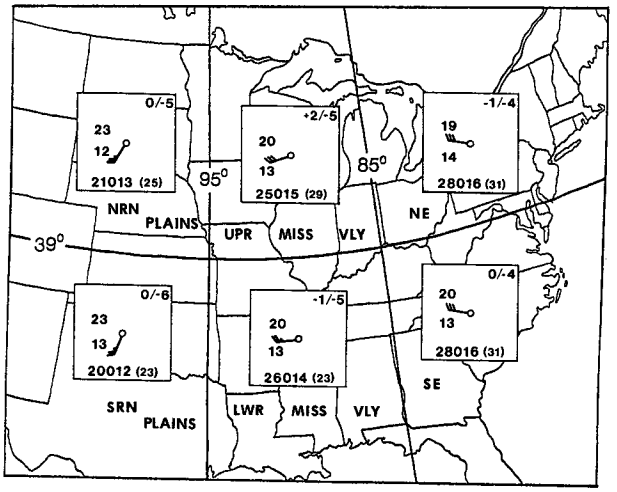

FIG. 3. Regional variations in the 850 mb parameters associated with NWF outbreaks. Relative to station circle, average temperature (°C) is to the left above, average dew point (°C) is to the left below, average wind direction and speed (m s^{-1} with knots in parentheses) is below, average Showalter Index for before beginning of outbreak (5A chart time) is to the upper right, left of the solidus, and average Showalter Index at temporal midpoint of outbreak is to the upper right, right of the solidus. Wind barb shows average wind direction and speed (full barb signifies 5 m s^{-1}).

This pattern is persistent enough that high values of low-level moisture frequently are carried into the westerly flow on the north side of the surface ridge. The amount of low-level moisture available may be enhanced further by transpiration from vegetation and by convergence along quasi-stationary frontal boundaries (see Sections 2e and 3). Thus, by July it is not unusual to have high values of low-level moisture in areas where the low-level flow has a north of west component.

c. Static stability with NWF outbreaks

The Showalter index (Showalter, 1953) and the total totals index (Miller, 1972) have been computed for all 163 cases, both for the antecedent conditions before the start of the outbreak (5A chart), and at the temporal midpoint of the outbreak.[6] The average Showalter index for "before" is near zero and the average total totals index is 47. However, there are wide variations in the pre-outbreak Showalter indices among individual cases. In about one-quarter (26%) of the cases, the Showalter indices prior to the beginning of the outbreaks are quite stable, with values greater than +2.

[5] Some of the differences between the values found for severe weather parameters in NWF situations and the results of other studies may be related to differences in the method of interpreting data. For example, David (1976) and Williams (1976) have interpolated data objectively by computer but the NWF data have been interpolated manually (see Schaefer and Doswell, 1979). Another factor that probably affects the parameter differences is the lack of a general outbreak data set for which direct comparisons can be made. Instead, comparisons are made with data based on tornado events only (David, 1976; Williams, 1976) and these events may be either isolated or part of an outbreak.

[6] 850 and 500 mb data were manually interpolated for the geographical midpoint of the outbreak for the times of the 5A chart, the 5B chart, and, when necessary, the chart 12 h after 5B. Then the data were interpolated further for the temporal midpoint of the outbreak. Finally, the interpolated 850 and 500 mb data were entered into a computer program (developed by Clarence David of NSSFC) that determined the Showalter and total totals indices.

TABLE 1. Percentage of NWF outbreaks within each region having temporal midpoints between 2230 and 1030 CST.

Region	Percent
Northern Plains	24
Upper Mississippi Valley	23
Northeast	13
Southeast	7
Lower Mississippi Valley	4
Southern Plains	4

The average Showalter index for the temporal midpoints of NWF outbreaks is −4.8 and the average total totals index is 54. Almost all NWF outbreaks (over 98%) have negative Showalter indices at the midpoint time and more than three-quarters of all cases (77%) have Showalter indices of −3 or lower. Since there is usually no decrease in the 500 mb temperatures during the course of an outbreak, it follows that a decrease in the Showalter index results from changes at the 850 mb level, especially moisture values. Examination of those cases in which the Showalter index starts out quite stable (greater than +2) indicates that high values of low level moisture are either present initially but below 850 mb, or are adjacent to (but not within) the outbreak area. Clearly, in the first instance, the moist layer deepens to the 850 mb level; whereas in the second, the moisture is advected into the outbreak area by the low-level flow.[7]

Geographically, Showalter indices for before the outbreaks begin show no recognizable pattern (Fig. 3). However, Showalter indices for the midpoint times generally indicate greater instability in the Plains states than in those areas farther east.

d. Surface parameters

NWF outbreak surface temperatures and dew points average higher than those associated with severe weather in general (Miller, 1972; Williams, 1976) emphasizing the "warm season" nature of NWF outbreaks. The average surface temperature for the temporal midpoints of the 163 NWF outbreak cases is 28.1°C and the average dew point is 19.4°C. Over two-thirds (67%) of all NWF cases are associated with surface temperatures of 26.7°C or above and surface dew points of 18°C or greater. Monthly averages for both temperature and dew point rise to distinct maxima in July. The July averages of 30.0°C for temperature and 21.1°C for dew point are 2.8°C and 2.2°C higher, respectively, than the July averages for tornadoes in general (Williams, 1976) (see Section 2b).

Twenty-five cases (15% of all cases) in the NWF data base have temporal midpoints in the diurnally cooler period between 2230 CST and 1030 CST (Table 1). However, 14 (56%) of these nighttime–early morning outbreaks are associated with surface temperatures of 23.9°C or more and most (84%) have midpoint temperatures of at least 21.1°C. Of the 138 cases with midpoints between 1030 and 2230 CST, over three-quarters (78%) are associated with temperatures of 26.7°C or more.

Sea level pressures associated with NWF outbreaks have a slightly higher average (1009.2 mb) than those for tornadoes in general (Williams, 1976), with three-quarters (75%) of the total NWF cases having pressures in the 1007 to 1015 mb range. Monthly averages with NWF outbreaks rise from 1007–1008 mb in May and June to above 1010 mb in July and August. These higher values are consistent with the weaker weather systems occurring during the summer months.

Figure 4 illustrates regional differences in NWF outbreak surface parameters. Note that the surface temperatures associated with NWF outbreaks in the Northern Plains and Upper Mississippi Valley regions average about 3°C lower than elsewhere. These lower readings may result partly from the relatively high percentage of nighttime outbreaks occurring in the north-central part of the United States (Table 1). The incidence of nighttime outbreaks in the other regions is much lower. Two other surface parameters showing patterns of regional variation are the dewpoint and the wind direction. Lower dewpoints in the Plains may be explained at least partially by higher elevations, while the southeasterly surface winds in the Plains regions are encouraged by the frequent development of low pressure troughs in the lee of the Rocky Mountains.

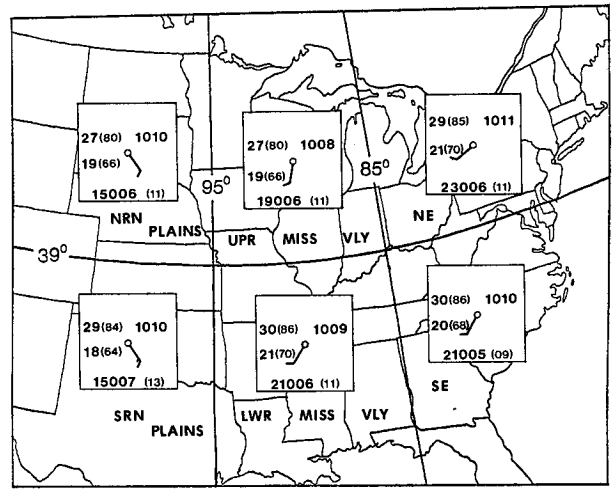

FIG. 4. Regional variations in the surface parameters associated with NWF outbreaks. Relative to station circle, average temperature (°C with °F in parentheses) is to the left above, average dew point (°C with °F in parentheses) is to the left below, average wind direction and speed (m s^{-1} with knots in parentheses) is below, and average sea level pressure (mb) is to the right above. Wind barb shows average wind direction and speed (full barb signifies 5 m s^{-1}).

[7] The Lifted Index (Galway, 1956) takes into account moisture values below 850 mb. However, due to computer changes at NSSFC, the data necessary to determine Lifted Indices values are not available for most of the period of this study.

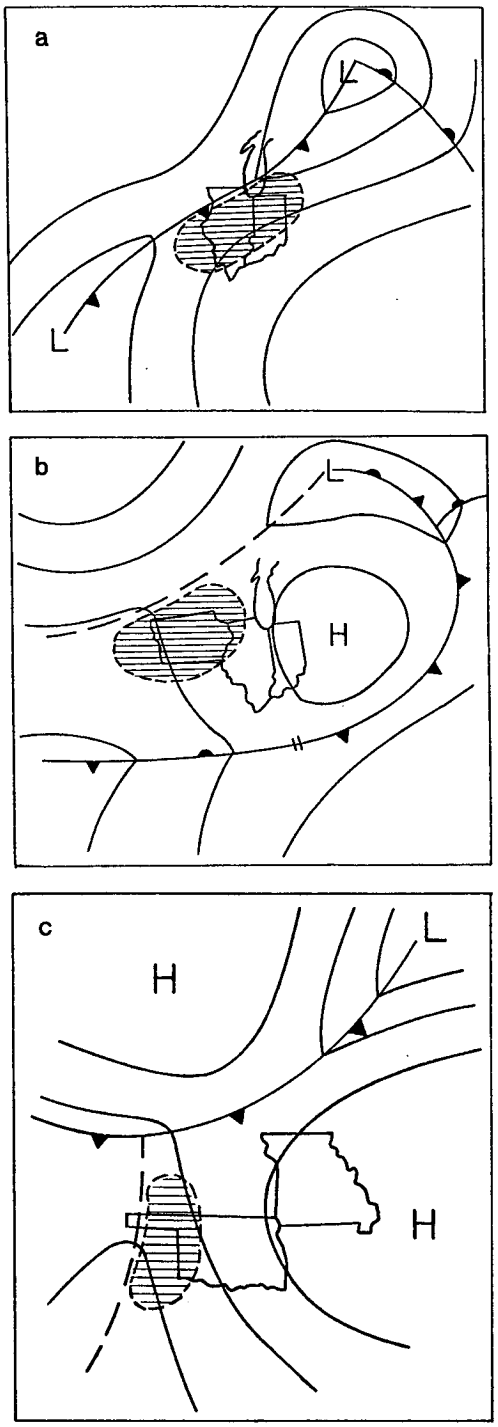

FIG. 5. Type G surface patterns. NWF outbreaks are indicated by hatched areas. Frontal symbols are conventional. (a) Type G1; (b) Type G2; (c) Type G3.

e. Surface patterns

Surface charts associated with all 163 outbreak cases have been used to identify six basic surface weather patterns (Figs. 5 and 6). These patterns fall into two general classes: those involving a NE–SW pressure trough system similar to Galway's (1958) model (the G patterns), and those involving a quasi-stationary front oriented generally in a WNW–ESE direction (the Q patterns). Frequency of occurrence is about equally divided between the G and Q classes.

Type G1 (Fig. 5a) is similar to Galway's mean surface chart. This pattern represents about 20% of the cases. G1 outbreaks almost always begin in the warm air mass ahead of the cold front and move southeastward.

Type G2 (Fig. 5b) is the most common surface pattern observed, occurring in 26% of the cases. This type resembles G1, with a surface low center well to the northeast of the outbreak area and an inverted trough to the southwest. However, the primary cold front in the G2 surface pattern has moved well east of the outbreak area, and the outbreak typically occurs in a modified continental polar air mass in which the low level temperature and moisture values are increasing. The relatively high frequency of this surface pattern is consistent with the finding by Notis and Stanford (1973) who observed that southeastward-moving (NWF) tornadoes "tend to occur behind the cold front." The G2 surface pattern is usually accompanied by a weak short-wave trough, typically identified by a wind maximum in the upper troposphere (500 mb level or higher), that is moving southeastward into the long-wave trough position. The surface reflection of this short-wave trough may only be an isallobaric couplet[8] and a weak wind shift line. It is typical for the ill-defined characteristics of the G2 pattern to become more like the G1 cold frontal pattern within the last few hours before the outbreak begins; i.e., the wind-shift line is associated with frontogenesis.[9]

Surface Type G3 (Fig. 5c) is rare, comprising only 3% of the cases, and has been observed to occur only in the Southern Plains. The surface pattern resembles Type G1. However, the outbreak occurs along the inverted lee trough line south of the cold front, rather than ahead of the front. There is usually no well-defined moisture discontinuity associated with the trough line.

Surface Type Q1 (Fig. 6a), occurring in 20% of the cases, is characterized by a quasi-stationary front extending eastward or southeastward from a low center well to the west or northwest of the outbreak area. The outbreak generally commences near the area where an axis of maximum surface wind intersects the quasi-stationary front.[10] Thus, the Q1 surface type is often

[8] Experience suggests the magnitude of the difference between the pressure rise center and fall center for a 2 h period is usually 2.5 mb or greater, with the distance between centers on the order of 240 to 280 km.

[9] There is more than a superficial resemblance between this post-frontal disturbance and the so-called polar low (e.g., Harrold and Browning, 1969; Reed, 1979).

[10] In situations involving the Q1 surface pattern and upslope low-level flow, the outbreak usually begins in the region of strongest upslope flow on the cool air side of the quasi-stationary boundary (see Doswell, 1980).

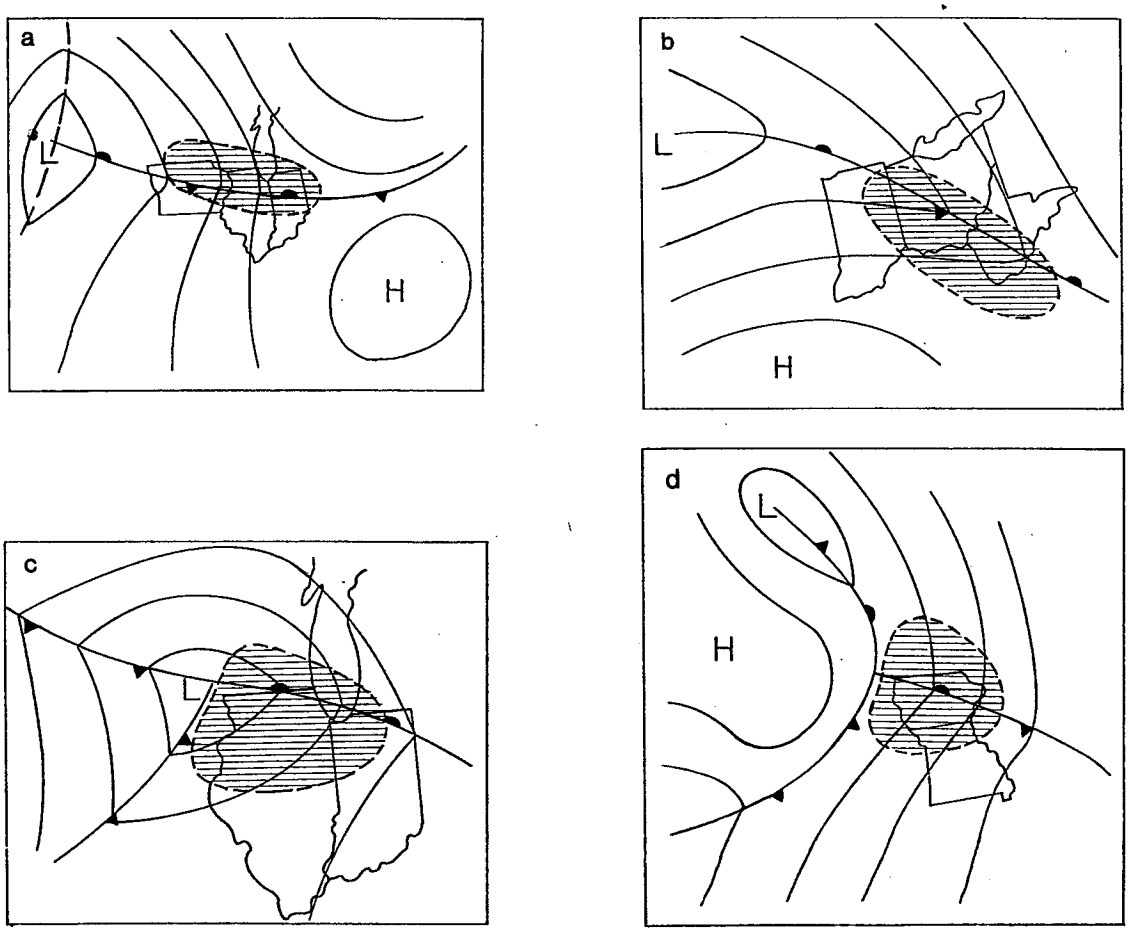

FIG. 6. Type Q surface patterns. (a) Type Q1; (b) Type Q1a; (c) Type Q2; (d) Type Q3.

similar to Miller's (1972) Type C synoptic pattern. The surface reflection of any associated short-wave trough aloft is usually best defined by an isoallobaric couplet (see footnote 8). The Type Q1a (Fig. 6b) surface pattern is a rare variation of the Q1 pattern (associated with 4% of the cases), observed only east of the Mississippi River. Type Q1a features a warm high pressure center located southwest of the outbreak area, causing the axis of maximum surface wind to intersect the stationary front from the west or northwest. Over 60% of the outbreaks with a Q1 surface pattern begin on the cool side of the stationary front.

Surface Type Q2 (Fig. 6c) occurs when a 500 mb short-wave trough, moving towards the long-wave trough position, is stronger than average (see Section 2f). A surface low center is associated with this trough and the outbreak occurs in the convergence zone near the low center. This surface type is present in 17% of all NWF outbreaks. While most of the Q2 outbreaks begin in the warm sector, more than one-quarter of them start in the cooler air mass north or northeast of the low center.

Surface Type Q3 (Fig. 6d) has an occluded low center northwest of the outbreak area. The outbreak takes place just to the east of the point of occlusion. This surface pattern is present in about 10% of the total cases and many of the outbreaks begin either in the cooler air north of the point of occlusion (44%) or along the frontal boundary extending eastward from the point of occlusion (25%).

Low-level air mass discontinuities induced by convective activity are an important influence in many severe weather situations (e.g., Miller, 1972; Purdom, 1976). In NWF situations, it is not unusual for such a boundary to be present in the outbreak area before the severe weather begins. The convective activity that created the boundary may have already dissipated. Examination of several NWF cases reveals that when such a boundary is present, a G type surface pattern may appear more like a Q type pattern with the activity boundary acting in the same manner as a quasi-stationary frontal boundary.

There are significant regional differences in the frequency distribution of the surface types (Table 2). The G2 surface pattern is the most common type in the Plains regions, accounting for almost half (49%) of all outbreaks in the Northern Plains. Generally, the frequency of the G2 pattern decreases toward the south-

TABLE 2. Frequency of surface types by region.

Surface type	Northern Plains	Upper Mississippi Valley	Northeast	Southern Plains	Lower Mississippi Valley	Southeast
Number of cases	37	47	15	24	25	15
% Q1	16	19	13	21	24	26.5
% Q1a	3	2	20	0	4	7
% Q2	8	28	7	8	20	26.5
% Q3	13	15	13	4	4	0
% G1	11	15	27	13	36	33
% G2	49	21	20	33	12	7
% G3	0	0	0	21	0	0
% Q	41	64	53	33	52	60
% G	59	36	47	67	48	40

east with fewer than 10% of the surface patterns associated with outbreaks in the Southeast region exhibiting G2 characteristics. The reverse pattern holds for G1 surface types. This suggests that any frontogenesis process taking place under NWF aloft is usually completed by the time the system reaches the Lower Mississippi Valley and Southeast regions.

The outbreak surface pattern most frequently occurring in the Upper Mississippi Valley region is the Q2 type, present in 28% of the area cases. In fact, almost half of all NWF outbreaks associated with the Q2 pattern occur in the Upper Mississippi Valley region. The Q2 surface pattern is also associated with a significant percentage of outbreaks occurring in the Southeast region (27%) and the Lower Mississippi Valley region (20%). However, a majority (56%) of the Q2 surface types in the southern two regions occur early in the NWF season, before 1 June. No Q2 surface types have occurred in the Lower Mississippi Valley region after June. At the same time over eight-tenths (85%) of the Q2 types occurring in the Upper Mississippi Valley region occur after May. Since the Q2 surface pattern is usually associated with the stronger 500 mb short-wave troughs (see Section 2f), this frequency shift northward during the summer months reflects the seasonal migration of the 500 mb polar jet.

The Q3 surface pattern is most common in the Northern Plains and Upper Mississippi Valley regions where 75% of all outbreaks associated with this type occur. However, the relative frequency of occurrence of the Q3 type is not high in either region (15% or less). The Q1 surface type is the most evenly distributed of the Q patterns, and, unlike the Q2 pattern, no well-defined geographical seasonal shift is noted.

Table 3 summarizes outbreak occurrences by surface weather pattern. Note the wide variation among the surface types of the air mass in which the severe weather begins. Outbreaks that commence in the warm air mass are likely to begin during the early to mid-afternoon hours. Almost two-thirds (66%) of the warm air mass cases begin between the hours of 1200 and 1600 CST. Outbreaks that begin in the cool air mass sector tend to start later in the afternoon, with more than half (55%) of the cool air mass cases beginning between 1400 and 1800 CST. Furthermore, those outbreaks that begin during the nighttime hours usually start in the cool air mass. Of the 21 outbreaks that began between 2000 and 0800 CST, only four were initiated solely in the warm sector. The tendency for nocturnal development to occur in the cool sector appears to be linked to a rather common synoptic pattern found with NWF outbreaks. About half (51%) of all NWF outbreaks are associated with a Q-type pattern. Fig. 3 suggests that outbreaks in the central United States are often accompanied by a southerly low-level jet. Sangster (1958) has shown that when a southerly

TABLE 3. Relative frequencies of NWF surface patterns and air mass of outbreak origin.

Surface type	Number of cases	Percent of all cases	Percent of cases commencing in cool sector	Percent of cases commencing in warm sector	Percent of cases commencing about same time in both air masses
G1	32	20	3	97	0
G2	43	26	86*	2	12
G3	5	3	0	100	0
Q1	32	20	63	28	9
Q1a	7	4	14	72	14
Q2	28	17	29	64	7
Q3	16	10	44	25	31

* Air mass anywhere north and west of primary cold front considered as cool sector.

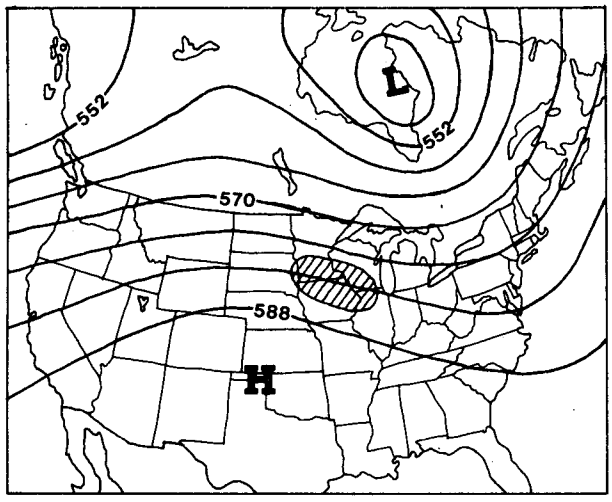

FIG. 7. Example of the basic NWF 500 mb pattern represented by a weak short-wave trough embedded in flow. Outbreak region indicated by hatched area.

low-level jet is present in the central United States and the jet intersects a generally east–west quasi-stationary front, a diurnal cycle of vertical motion (700 mb) develops along and to the north of the front in the cool air mass. Positive (upward) vertical motion develops in the late afternoon hours and reaches a peak about 2100–0000 CST. The contribution by this source of positive vertical motion may explain the initiation of severe weather outbreaks that are out of phase with the diurnal heating cycle. Also, the nighttime maximum in upward vertical motion is probably the main reason why NWF episodes occurring in the Northern Plains are often prolonged into the early morning hours (Johns, 1982b).

f. Variations in the NWF 500 mb pattern

The criteria for defining NWF outbreaks (Johns, 1982b) and the 500 mb parameter climatology (Section 2a) suggest a basic NWF 500 mb pattern similar to that shown in Fig. 7. However, differences from this basic pattern frequently occur, and the 163 cases in this study have been examined to determine synoptic characteristics that are of significance to the forecaster. Table 4 illustrates the more important variations.

Well-defined, digging 500 mb short-wave troughs, similar to the one shown in Fig. 8, are present with almost half (43%) of all NWF outbreaks. This type of 500 mb pattern is especially common with the G1 and Q2 surface types, occurring with 68% and 64% of all such cases, respectively. However, this "strong digging short-wave trough" pattern occurs with only 35% of the G2 surface types and 18% of the Q1 types. These statistics appear reasonable since stronger 500 mb short-wave troughs are more likely to be associated with a well-defined cold front (G1) rather than a trough line (G2), or a closed surface low (Q2) rather than a quasi-stationary front (Q1). In most cases involving the G2 and Q1 surface patterns then, upper-level short-wave troughs are usually weak and low-level warm advection is probably a critical factor in providing the necessary vertical motion for severe weather development (see Section 2b).

About one-fifth (21%) of all NWF outbreaks are associated with the southern branch of a split 500 mb flow pattern, shown schematically in Fig. 9. This pattern tends to occur early in the NWF season, with 62% of all such cases occurring before July. The amplitudes of the short-wave troughs in the southern branch cases vary from very low (as in Fig. 7) to high (as in Fig. 8). Nearly all (80%) of the G3 surface types are associated with this 500 mb pattern.

It was noted in Section 2a that only 12% of all NWF outbreaks have severe reports occurring north of the 500 mb jet. Inspection of the 500 mb patterns associated with these 19 cases reveals that a majority (63%) occur with a strong digging short-wave trough (Fig. 8). Almost all such cases (89%) occur either with a strong digging short-wave trough or in the southern branch of a 500 mb split flow pattern. There is also a tendency for "north of the jet" severe activity to occur early in the NWF season, with almost two-thirds (63%) of such cases occurring before July.

About 10% of all NWF cases occur in the broad cyclonic flow around a large, intense 500 mb trough (Fig. 10). More than three-quarters (77%) of all out-

TABLE 4. Frequency of 500 mb features associated with NWF surface patterns.

Surface pattern	Cyclonic flow	Anti-cyclonic flow	Dif-fluence	Wind maximum east of meridian through midpoint	Wind maximum 550 km or more distant from midpoint	Strong digging short wave	Southern branch of split flow	Broad cyclonic flow
G1	55	45	47	19	42	68	10	6
G2	65	35	42	26	21	35	19	23
G3	60	40	20	0	40	0	80	0
Q1	52	48	22	27	18	18	24	6
Q1a	57	43	86	14	14	57	14	0
Q2	75	25	29	18	21	64	29	7
Q3	25	75	25	25	38	38	13	0
All cases	58	42	36	22	26	43	21	10

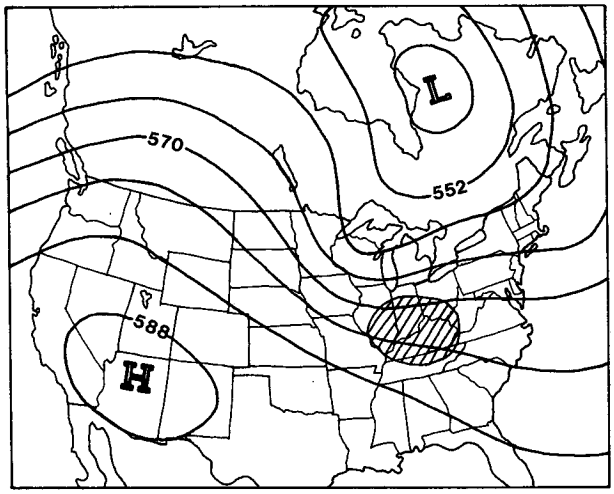

FIG. 8. Example of a NWF 500 mb pattern exhibiting a strong digging short-wave trough. Outbreak region indicated by hatched area.

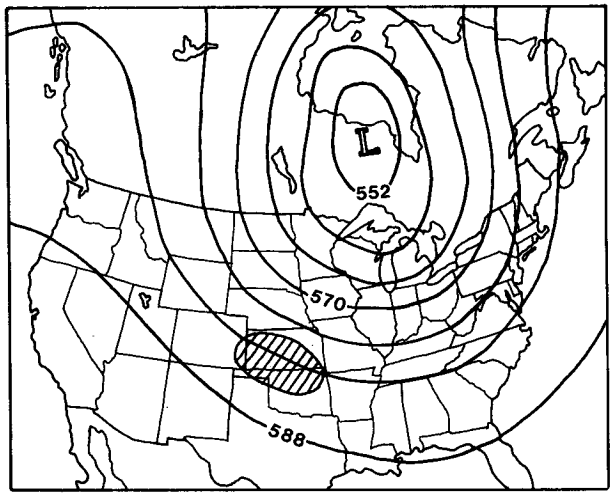

FIG. 10. Example of a NWF 500 mb broad cyclonic flow pattern. Outbreak region is indicated by hatched area.

breaks exhibiting this flow pattern occur in July and August. Almost one-quarter (23%) of those outbreaks with the G2 surface pattern occur with this type of 500 mb flow (see footnote 9).

Approximately one-third (36%) of all NWF outbreaks occur beneath areas of diffluence at 500 mb. Diffluence is more common in situations involving G type surface patterns (41%) than it is with the Q type patterns (30%). Diffluence is associated with almost one-half (47%) of all outbreaks involving the G1 surface pattern.

Curvature of the 500 mb flow at the temporal midpoint of an outbreak is cyclonic in 58% of all NWF cases. Cyclonic flow is most common with Q2 patterns (75%) and G2 patterns (65%) and least common with Q3 patterns (25%). An examination of the 500 mb charts associated with Q3 surface patterns reveals a tendency for the outbreaks to occur well ahead of a short-wave trough (of moderate or greater amplitude) and near the short-wave ridge line. Hence, these outbreaks often occur in an area of anticyclonic flow as the example in Fig. 11 shows.

Table 4 illustrates variations in the locations of the 500 mb wind maxima (relative to the outbreak centerpoint) associated with the different surface types. The wind maxima tend to be farthest away from the centerpoint when G1, G3 and Q3 surface patterns are present. About 40% of such cases have the wind maxima at a distance of 550 km (300 nm) or more from the outbreak centerpoint. There is generally little vari-

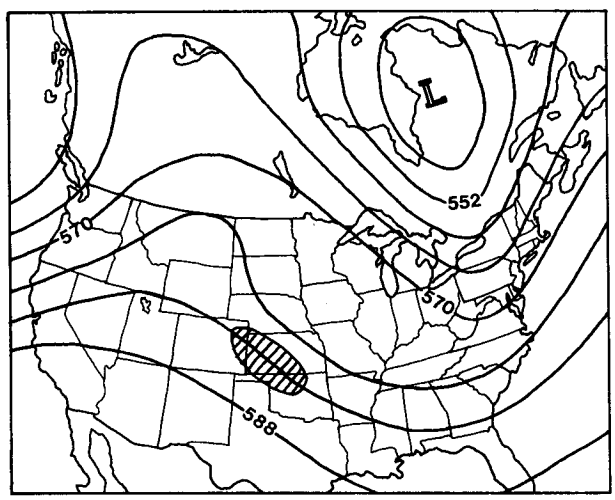

FIG. 9. Example of a NWF 500 mb split flow pattern with outbreak occurring in the southern branch. Outbreak region is indicated by hatched area.

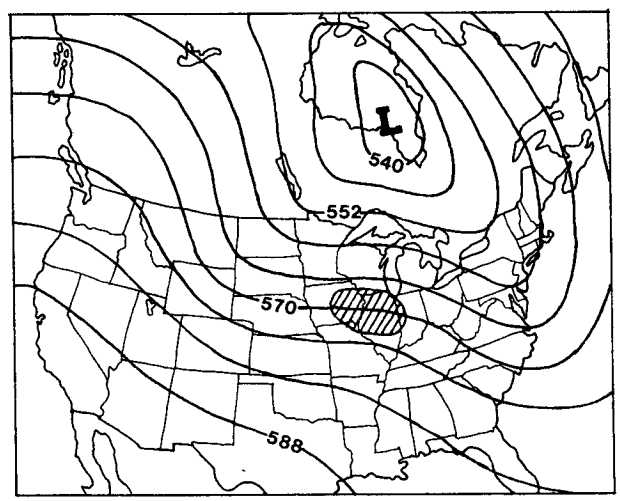

FIG. 11. Example of a typical NWF 500 mb pattern accompanying a Q3 surface pattern. Outbreak region is indicated by hatched area.

ation in the directions of the maxima from the centerpoint among the various surface types. The lone exception is the G3 surface pattern, for which all maxima are located west of the meridian passing through the centerpoint.

3. The origins of the A1 and A2 high-frequency axes

Johns (1982b) has shown that NWF outbreaks occur most often along two axes, denoted A1 and A2 (Fig. 12). The A2 axis coincides well with the primary tornado axis, oriented in a NNE–SSW direction through the central Plains (Kelly *et al.*, 1978). However, the primary NWF high frequency axis, A1, lies nearly perpendicular to the A2 axis and has highest frequencies well to the east of the Plains states.

The existence of the A1 axis appears to be related to the mean 500 mb flow pattern and a favored polar frontal position during the summer months. The criteria for NWF outbreaks require a stable long-wave pattern during the course of an outbreak. Furthermore, since most such outbreaks are part of a series (Johns, 1982b), it can be inferred that the long-wave pattern often remains stable for a period of days as NWF outbreaks continue to take place. Such a persistent pattern appears to be representative of the mean 500 mb flow pattern that becomes established during the summer months.

Figure 13 illustrates how the mean 500 mb flow pattern over the United States undergoes a significant change in the late spring. From a split flow pattern in May, the mean flow pattern evolves into one with a long-wave ridge over western North America, a long-wave trough near the east coast of North America, and a single broad band of west-northwesterly flow covering much of Canada and the northern United States east of the Rocky Mountains. This mean pattern persists through the summer season, the time of peak NWF outbreak activity. Since short-wave troughs associated with NWF outbreaks generally produce only minor distortions to the long-wave pattern, it follows that individual NWF outbreaks usually occur not far from the mean jet position with a long axis oriented parallel to the mean upper flow. Thus, during the course of a NWF season, one expects a band of higher NWF outbreak frequency to occur between the upstream mean ridge and the downstream mean trough positions, close to the mean jet and oriented parallel to it. Note how the A1 high-frequency axis (Fig. 12) tends to fit this pattern.

Close examination of the A1 axis reveals that it is generally located to the south of the mean summer position of the 500 mb jet. The axis also appears to curve around the Great Lakes. These two characteristics are apparently linked to a favored position of the polar front during the NWF season. The NWF data base shows that a large majority (64%) of the outbreaks occurring in the Upper Mississippi Valley region are associated with a quasi-stationary frontal boundary oriented generally WNW–ESE. Most of the

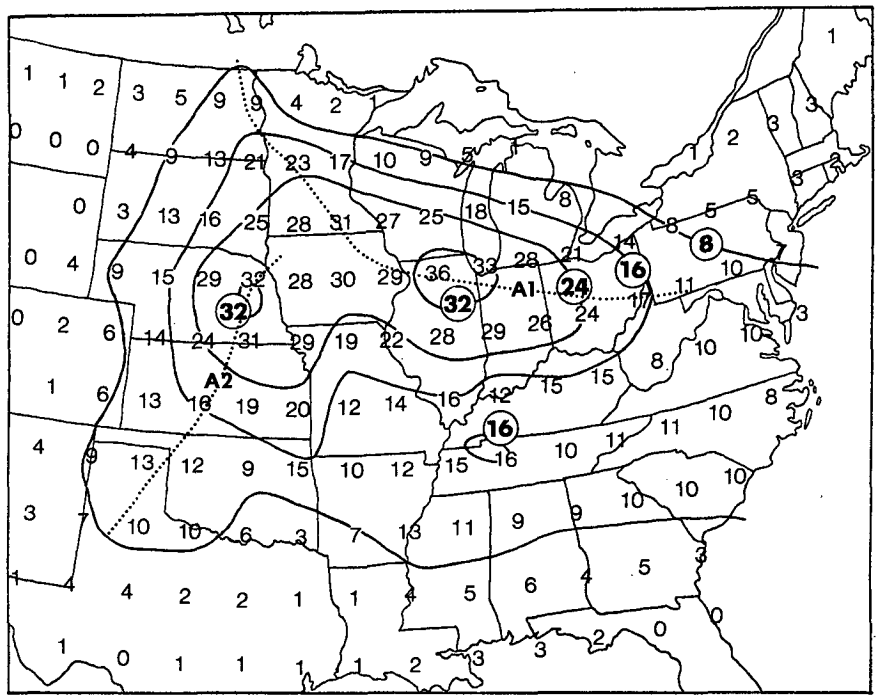

FIG. 12. Total number of northwest flow outbreaks occurring in 2° Marsden squares for the period 1962–77. A1 and A2 high-frequency axes are indicated by dotted lines (from Johns, 1982b).

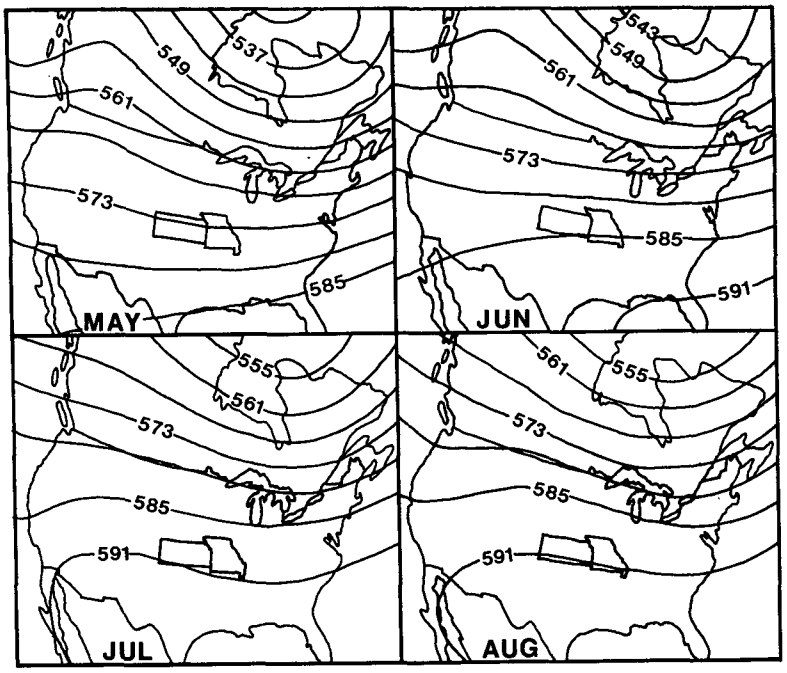

FIG. 13. Mean monthly 500 mb heights (dam) for May, June, July and August (from Normal Weather Charts, Tech. Paper No. 21, U.S. Weather Bureau).

A1 high frequency axis lies within this area. Furthermore, NWS forecasters at both Milwaukee and Chicago[11] have long noticed that in the spring and early summer slowly moving cold fronts have a strong tendency to move to the south end of Lake Michigan before becoming stationary. Hence, the relatively cold water of Lake Michigan, and more generally of the Great Lakes, acts as a source for anticyclogenesis often forcing quasi-stationary frontal boundaries to lie along the southwestern periphery of the Great Lakes region. The A1 axis, then, reflects the most common position of this frontal boundary at the time when NWF outbreaks are taking place.

Since most NWF outbreaks take place beneath and/or south of the 500 mb jet axis, the data in Fig. 1 suggest that a significant number of outbreaks take place in the right front quadrant relative to the 500 mb wind maxima, not the classical pattern for severe weather development (Beebe and Bates, 1955; Newton and Newton, 1959). An examination of several individual cases reveals that this is indeed the case. However, in these same outbreak cases strong conditional instability was present and pronounced low-level warm advection was taking place, especially in the initial stages of each outbreak. Maddox and Doswell (1982) have suggested that in some cases low-level warm advection is the key factor in providing sufficient upward vertical motion to release the instability. Therefore, in many of the NWF cases it may be that an *approaching* 500 mb short-wave trough induces backing of the low-level wind field along a quasi-stationary boundary (Q surface pattern) setting up a significant warm advection field beneath the right front quadrant relative to the 500 mb wind maximum (Uccellini and Johnson, 1979). And with the presence of high values of conditional instability, intense convection commences. This theory helps to explain the role of the mean polar frontal boundary in determining the location of the A1 high frequency axis.

The A2 high-frequency axis is likely a result of several factors related to the topography of the region. Enhanced wind shear due to the presence of the Rocky Mountains is one contributor (See Section 4). Another concerns low-level moisture distribution. Examination of several individual cases suggests that in most NWF outbreak situations in the Plains regions high values of low-level moisture are usually restricted to a relatively narrow north–south tongue. This pattern often represents the northward return of low-level moisture in the wake of a southeastward moving continental polar airmass.[12] Consequently, in such situations, the eastward development of outbreak activity from the Plains states is limited.

A third contributor to the A2 axis appears to be the effect of upslope low-level flow. Some of the cases examined above occurred with a Q1 surface pattern in

[11] Personal communication with Richard Koeneman, WSFO, Milwaukee and Henry Yario, WSFO, Chicago.

[12] This type synoptic pattern is consistent with the high frequency of G2 surface patterns in the Plains regions.

TABLE 5. Average wind shear between 850 and 500 mb associated with tornadoes in general (after David, 1976) and with NWF outbreaks. Wind speeds are in meters per second with knots in parentheses.

	Average 850 mb wind		Average 500 mb wind		850–500 mb directional shear	850–500 mb speed shear
	Direction	Speed	Direction	Speed		
Tornadoes occurring in Jan., Feb., Mar.	220	13 (26)	235	26 (50)	15°	13 (24)
Maxi-tornadoes	218	10 (20)	240	21 (41)	22°	11 (21)
All tornadoes	216	8 (16)	241	16 (32)	25°	8 (16)
Tornadoes occurring in June–August	223	6 (11)	256	11 (22)	33°	5 (11)
NWF outbreaks	241	14 (27)	298	15 (30)	57°	1 (3)

which the severe weather developed on the north side of the frontal boundary in upslope (easterly) flow. The 500 mb flow was generally weaker than average for NWF situations. These cases fit the typical Doswell (1980) High Plains severe weather pattern with pronounced directional wind shear and lifting primarily due to upslope low-level flow. Once initiated, some of these cases formed a mesoscale convective complex (Maddox, 1980) which propagated through the low-level moist axis at lower elevations.

4. The role of directional shear in NWF outbreaks

Severe weather events occur under a variety of mesoscale conditions. Isolated, quasi-random events of hail and/or wind gusts can occur from any thunderstorm or cluster of thunderstorms when a locally favorable vertical profile of temperature and moisture is attained (Miller, 1972). However, an *organized pattern* of severe weather events generally occurs with a self-perpetuating storm system (Marwitz, 1972a, b, c; Browning, 1977; Fujita, 1978, 1981). And in order to maintain a severe local storm system, a continuous and sufficiently strong low-level relative inflow of conditionally unstable air is necessary (Newton, 1950; Marwitz, 1972b; Browning, 1977).

The low-level inflow relative to a storm system is related to the vertical environmental wind shear (Newton, 1963). Most storm cells move with a velocity nearly the same as that of the mean environmental wind (Byers and Braham, 1949; and others). However, some storm systems, especially self-perpetuating types, tend to move or propagate with a velocity that deviates from the mean environmental wind (Newton and Katz, 1958; Browning and Ludlam, 1962; Browning, 1964; Johns and Hirt, 1983; and others). The deviation of storm motion from the mean environmental flow varies considerably among individual cases (Darkow and McCann, 1977; Johns and Hirt, 1983). However, despite these wide variations, the data supplied by the aforementioned researchers suggest that the contribution to low-level relative inflow generated by deviant storm motion is usually less than the contribution due to non-deviant motion. Thus, it follows that the value of the low-level inflow due to environmental wind shear is often an important factor in the maintenance of self-perpetuating storm systems.

In the absence of mean environmental wind data, an approximation of the environmental wind shear can be obtained by computing the shear between 500 and 850 mb.[13] The tornado proximity soundings presented by Darkow and McCann (1977) indicate that the 500 mb wind vector is usually very similar to the mean environmental wind vector in tornadic situations. The nature of the low-level relative inflow into severe storms indicates that the 850 mb surface generally lies above the level of strongest relative inflow, except perhaps in the High Plains (Bonner, 1968; Fankhauser, 1976). Therefore, the mean low-level maximum inflow vector usually is below 850 mb and backed relative to the 850 mb wind. This implies that the 850–500 mb contribution to shear generally is an underestimate of the total shear, but still a reasonable approximation.

Table 5 suggests that the nature of the environmental wind shear associated with severe local storms changes considerably during the severe weather season. Late winter and early spring severe weather situations, which include most of the violent tornadoes (Kelly *et al.*, 1978), generally are associated with relatively large values of speed shear and relatively small values of directional shear (McNulty, 1978). As summer approaches, there is a general decrease in atmospheric wind speeds, and the speed contribution to wind shear in severe weather situations decreases accordingly. However, at the same time, the directional contribution to shear becomes larger. Consequently, the continuation of severe weather occurrences into the late spring and summer is aided by the ability of thunderstorms to develop in areas where the directional contribution to vertical shear offsets the general decrease in the speed contribution. The examples of High Plains outbreaks presented by Doswell (1980) and the NWF outbreak of 28 June 1979 (Johns, 1979) clearly demon-

[13] Only standard level radiosonde data were available for the NWF data base.

strate the importance of directional shear in summertime situations. Table 5 suggests that for NWF outbreaks in general, the directional contribution to environmental wind shear is a major factor in providing sufficient relative inflow for severe storm maintenance. Note also that the veering of the environmental wind with height implies warm advection within the 850–500 mb layer (Holton, 1979). This result is in accord with the discussion in Section 2b indicating the presence of pronounced low-level warm advection in the genesis region of many NWF outbreaks.

From Table 6 it appears that, for both NWF outbreaks and severe weather in general, the directional contribution to environmental wind shear plays a greater role in the Great Plains region than in areas farther east. This pattern appears to result from the topography of the United States. That is, the mid-latitude westerlies tend to develop leeside troughs east of the Rocky Mountains and a southerly low-level flow frequently develops in response through the Great Plains (Palmén and Newton, 1969; Doswell, 1982). This flow is often enhanced by the seasonal shift of the subtropical high and the sloped terrain of the Great Plains region (Uccellini and Johnson, 1979; and others). The resulting high values of directional shear apparently compensate for the proximity of the 500 mb long-wave ridge and the associated lower 500 mb wind speeds (see Section 2a).

5. Summary and conclusions

Examination of the synoptic patterns associated with NWF outbreaks reveals that such episodes cannot be viewed as a simple clockwise rotation of the patterns attending the classical southwesterly flow (SWF) outbreak situation. It appears that most of the differences between NWF and SWF parameters and patterns stem from differences in their respective seasonal frequencies. SWF outbreaks can occur any time of year. However, the most significant episodes occur in the late winter and spring and are usually characterized by strong well-defined jet streams and intensifying baroclinic weather systems. NWF outbreaks, on the other hand, are mostly restricted to the summer months when low-level moisture is widespread, and can be more easily advected into areas beneath NWF at 500 mb. Hence, NWF outbreaks are associated with the strong thermodynamic parameters typical of the summer season.

The seasonal changes in the values and distribution of the severe weather parameters appear to have a significant effect on the meteorological patterns associated with severe weather outbreaks. In the strong baroclinic situations of winter and spring (usually SWF), the location of an outbreak is often dictated by the position and orientation of the mid-tropospheric (or higher level) jet (Beebe and Bates, 1955; Newton and Newton, 1959; and others). The NWF data set suggests that in the strong thermodynamic situations of summer, the mid-tropospheric (or higher level) jet often plays an indirect role, with surface boundaries and low-level warm advection being key factors in determining outbreak location. Thus, it may be that the primary mechanism for triggering severe weather outbreaks varies with the season.

It has been determined that NWF outbreaks tend to occur along either of two high-frequency axes, A1 and A2 (Fig. 12), and explanations for the locations of these axes have been presented (see Section 3). Close examination of Fig. 12 reveals other interesting features in the frequency distribution. However, the significance of most of these features is questionable due to the relatively small size of the data sample. A possible exception to this may be the relative frequency maximum over western Tennessee, northern Mississippi and extreme eastern Arkansas. The reason for this maximum is not clear. However, one might speculate that under NWF conditions the topography of the Ozark Plateau distorts the low-level wind and moisture fields in such a way as to enhance the development of severe weather activity over the adjacent portions of the Mississippi Valley.

TABLE 6. Average wind shear between 850 and 500 mb associated with tornadoes in general (after David, 1976) and with NWF outbreaks. Regional variations indicated by grouping NWF regional data with closest comparable geographical region, as defined by David (1976), for general tornadoes. Wind speeds are in meters per second with knots in parentheses.

	Average 850 mb wind		Average 500 mb wind		850–500 mb directional shear	850–500 mb speed shear
	Direction	Speed	Direction	Speed		
NWF Southern Plains	200	12 (23)	299	12 (24)	99°	0 (1)
David's Region 3 tornadoes	192	6 (12)	251	9 (18)	59°	3 (6)
NWF Northern Plains	210	13 (25)	296	15 (30)	86°	2 (5)
David's Region 2 tornadoes	225	5 (10)	255	13 (26)	30°	8 (16)
NWF Upper Mississippi Valley	250	15 (29)	297	17 (33)	47°	2 (4)
David's Region 5 tornadoes	247	8 (16)	260	14 (27)	13°	6 (11)
NWF Northeast	280	15 (30)	295	17 (34)	15°	2 (4)
David's Region 6 tornadoes	256	10 (19)	258	15 (30)	2°	5 (11)

The work of other researchers (Darkow and McCann, 1977; and others) suggests that environmental wind shear is an important factor in severe thunderstorm development. Furthermore, synoptic parameters associated with both NWF outbreaks and tornadoes in general (David, 1976) imply that the nature of environmental wind shear in severe weather situations changes considerably with the season and with the geographical area. Generally, these variations involve differences in the directional and speed contributions to the shear vector. Winter and early spring severe weather outbreaks usually involve a large speed contribution to shear. The low-level wind speeds can vary from weak (Branick, 1981) to very strong (Johns, 1982a). As the severe weather season progresses, the speed contribution to shear decreases while the directional contribution increases. NWF outbreaks, then, are usually associated with large directional and small speed contributions to the wind shear vector. The many variations in the form of the environmental wind shear make it difficult to evaluate the general magnitude by visual inspection. It would be advantageous to develop objective analyses of the environmental wind shear. However, as Doswell and Lemon (1979) have suggested, the upper-level winds aloft data operationally available to forecasters are difficult to use for extrapolating the shear fields.

Finally, operational meteorologists might evaluate the potential for NWF severe thunderstorm outbreaks in their forecast areas by developing a checklist, perhaps similar in format to the one developed by Gulezian (1980) for New England severe thunderstorms. (Tables 7 and 8 have been provided for this purpose.) Such a NWF checklist might include the following parameters and patterns:

Monthly frequency (Johns, 1982b)
Diurnal frequency (Johns, 1982b and Table 1)
Surface temperature (Section 2d and Table 7)
Surface dew point (Section 2d and Table 7)
Surface pressure (Section 2d and Table 8)
Surface pattern (Sections 2e and 2f; Tables 2, 3, and 4; Figs. 5a–c and 6a–d)
Convective activity boundaries (Section 2e)
850 mb temperature (Section 2b and Table 7)
850 mb dew point (Section 2b and Table 7)
850 mb wind speed and direction (Section 2b and Table 7)
850 mb thermal advection (Section 2b)
Showalter Index (Section 2c and Table 8)

TABLE 7. For each region, minimum parameter values associated with at least 50, 75 or 90% of all NWF outbreaks occurring in that region. Temperatures and dew points in degrees Celsius with degrees Fahrenheit in parentheses. Wind speeds in meters per second with knots in parentheses.

Percentage of outbreaks	Southern Plains	Northern Plains	Lower Mississippi Valley	Upper Mississippi Valley	Southeast	Northeast	Parameter
90	24 (75)	24 (76)	24 (75)	22 (72)	27 (80)	28 (82)	Surface temperature between
75	28 (82)	27 (80)	27 (80)	26 (79)	27 (81)	28 (83)	1030 and 2230 CST
50	29 (85)	29 (84)	31 (88)	29 (85)	31 (88)	30 (87)	
90	*	19 (66)	*	20 (68)	*	*	Surface temperature between
75	*	21 (70)	*	23 (73)	*	*	2230 and 1030 CST
50	*	23 (74)	*	26 (78)	*	*	
90	15 (60)	15 (60)	17 (63)	15 (59)	15 (60)	18 (65)	Surface dew point
75	16 (62)	17 (63)	20 (68)	17 (63)	18 (64)	20 (68)	
50	17 (63)	20 (68)	22 (72)	20 (68)	20 (68)	21 (70)	
90	19	19	16	16	17	17	850 mb temperature
75	21	21	19	18	18	17	
50	23	24	20	21	21	20	
90	11	8	12	8	10	11	850 mb dew point
75	11	10	13	11	12	13	
50	13	12	13	13	13	13	
90	8 (15)	8 (15)	10 (20)	8 (15)	10 (20)	13 (25)	850 mb wind speed
75	10 (20)	10 (20)	10 (20)	13 (25)	13 (25)	13 (25)	
50	13 (25)	13 (25)	13 (25)	15 (30)	18 (35)	18 (35)	
90	8 (15)	10 (20)	10 (20)	10 (20)	8 (15)	13 (25)	500 mb wind speed
75	10 (20)	13 (25)	13 (25)	13 (25)	13 (25)	15 (30)	
50	13 (25)	15 (30)	13 (25)	15 (30)	13 (25)	15 (30)	
90	18 (35)	18 (35)	21 (40)	23 (45)	21 (40)	23 (45)	500 mb speed of wind
75	21 (40)	21 (40)	23 (45)	26 (50)	26 (50)	23 (45)	maximum
50	21 (40)	26 (50)	28 (55)	31 (60)	28 (55)	26 (50)	

* Denotes insufficient data sample.

TABLE 8. For each region, maximum parameter values associated with at least 50, 75 or 90% of all NWF outbreaks occurring in that region. Pressures in millibars and temperatures in degrees Celsius.

Percentage of outbreaks	Southern Plains	Northern Plains	Lower Mississippi Valley	Upper Mississippi Valley	Southeast	Northeast	Parameter
90	1013	1013	1012	1013	1014	1015	Surface pressure
75	1012	1011	1011	1011	1013	1013	
50	1010	1009	1010	1008	1011	1011	
90	−9	−8	−7	−7	−7	−7	500 mb temperature
75	−10	−9	−8	−8	−7	−9	
50	−11	−11	−10	−10	−9	−10	
90	−2	−3	−1	−1	0	−1	Showalter Index
75	−4	−3	−3	−3	−2	−2	
50	−5	−5	−4	−4	−3	−3	

500 mb temperature (Section 2a and Table 8)
500 mb wind speed (Table 7)
500 mb wind speed maximum (Section 2a and Table 7)
500 mb wind maximum location (Section 2a and Fig. 1)
500 mb pattern (Section 2f; Table 4; Figs. 7–11)
Synoptic scale vertical wind shear (Tables 5 and 6).

In addition to the NWF data listed above, a forecaster should consider regional effects, such as upslope flow (Doswell, 1980), and general severe weather forecasting aids which could apply in NWF situations, for example, 700 mb dry intrusions (see Miller, 1972). Experimentation with a NWF checklist developed from the NWF data set, regional guidelines, and applicable general severe weather forecasting aids could lead to more accurate forecasts of summertime severe weather.

Acknowledgments. This study was partially funded under Interagency Agreement RES-76-106 between the Office of Nuclear Regulatory Research, Nuclear Regulatory Commission and the National Severe Storms Forecast Center, National Weather Service, NOAA. The author is especially grateful to Dr. Charles A. Doswell III (currently at NOAA's Environmental Research Laboratory) for his encouragement in the completion of the project and for his many beneficial suggestions for improving the manuscript, and to Beverly D. Lambert for the many hours of typing necessary to arrive at the final product. The author also wishes to thank Dr. Joseph T. Schaefer of the SSD, NWS Central Region, and Dr. Richard L. Livingston, Carolyn M. Kloth and Steven J. Weiss of NSSFC as well as Clifton W. Green and Edward A. Jessup of the National Weather Service Unit at the FAA Academy for their suggestions. The work done by the NSSFC computer staff and logistical support of Sidney Cornell and Bill Henry is gratefully appreciated.

REFERENCES

Beebe, R. G., and F. C. Bates, 1955: A mechanism for assisting in the release of convective instability. *Mon. Wea. Rev.*, **83**, 1–10.

Bonner, W. D., 1968: Climatology of the low level jet. *Mon. Wea. Rev.*, **96**, 833–850.

Branick, M. L., 1981: Meteorological analysis of a severe supercell thunderstorm over southern Mississippi, 31 March 1981. Southern Topics, July 1981, National Weather Service Southern Region, Ft. Worth, 7 pp. [Available from Sci. Ser. Div., Southern Region Office, NWS, 10E09 Federal Building, 819 Taylor Street, Ft. Worth, TX 76102.]

Browning, K. A., 1964: Airflow and precipitation trajectories within severe local storms which travel to the right of the winds. *J. Atmos. Sci.*, **21**, 634–639.

——, 1977: The structure and mechanisms of hailstorms. *A Review of Hail Science and Hail Suppression. Meteor. Monogr.*, No. 38, Amer. Meteor. Soc., 1–39.

——, and F. H. Ludlam, 1962: Airflow in convective storms. *Quart. J. Roy. Meteor. Soc.*, **88**, 117–135.

Byers, H. R., and R. R. Braham, Jr., 1949: *The Thunderstorm.* U.S. Govt. Printing Office, 287 pp.

Darkow, G. L., and D. W. McCann, 1977: Relative environmental winds for 121 tornado bearing storms. *Preprints 10th Conf. Severe Local Storms,* Omaha, Amer. Meteor. Soc., 413–417.

David, C. L., 1976: A study of upper air parameters at the time of tornadoes. *Mon. Wea. Rev.*, **104**, 540–545.

——, 1977: A study of synoptic conditions associated with New England tornadoes. *Preprints 10th Conf. Severe Local Storms,* Omaha, Amer. Meteor. Soc., 180–185.

Doswell, C. A., III, 1980: Synoptic-scale environments associated with high plains severe thunderstorms. *Bull. Amer. Meteor. Soc.*, **61**, 1388–1400.

——, 1982: The Operational Meteorology of Convective Weather. Vol. I: Operational Mesoanalysis. NWS NSSFC-5 Tech. Memo., 162 pp. [Available from National Severe Storms Forecast Center, Room 1728, 601 E. 12th St., Kansas City, MO 64106.]

——, and L. R. Lemon, 1979: An operational evaluation of certain kinematic and thermodynamic parameters associated with severe thunderstorm environments. *Preprints 11th Conf. Severe Local Storms,* Kansas City, Amer. Meteor. Soc., 397–402.

Fankhauser, J. C., 1976: Structure of an evolving hailstorm. Part II: Thermodynamic structure and airflow in the near environment. *Mon. Wea. Rev.*, **104**, 576–587.

Fujita, T. T., 1978: Manual of downburst identification for project NIMROD. Satellite and Mesometeorology Res. Pap. No. 156, University of Chicago, 104 pp.

——, 1981: Tornadoes and downbursts in the context of generalized planetary scales. *J. Atmos. Sci.*, **38**, 1511–1534.

Galway, J. G., 1956: The lifted index as a predictor of latent instability. *Bull. Amer. Meteor. Soc.*, **37**, 528–529.

——, 1958: Composite charts for tornado situations under northwest flow aloft. *Preprints General Meeting,* Kansas City, Amer. Meteor. Soc., 23 pp. [Available from National Severe Storms Fore-

cast Center, NWS, Room 1728, 601 E. 12th St., Kansas City, MO 64106.]

Giordano, L. A., and J. M. Fritsch, 1983: Northwest flow: The most common upper level flow for summertime tornadoes in the mid-Atlantic states. *Preprints 13th Conf. Severe Local Storms,* Tulsa, Amer. Meteor. Soc., 136–141.

Gulezian, D. P., 1980: Severe weather checklist used at National Weather Service Office, Portland, Maine. *Bull. Amer. Meteor. Soc.,* **61,** 1592–1597.

Harrold, T. W., and K. A. Browning, 1969: The polar low as a baroclinic disturbance. *Quart. J. Roy. Meteor. Soc.,* **95,** 710–723.

Holton, J. R., 1979: *An Introduction to Dynamic Meteorology.* Academic Press, pp. 68–71.

Johns, R. H., 1979: The severe thunderstorm outbreaks of June 28 and 29, 1979, Technical Attachment 79-10. Central Region News and Views, NWS, Kansas City, 6 pp. [Available from Sci. Ser. Div., Central Region Office, NWS, Room 1747, 601 E. 12th St., Kansas City, MO 64106.]

——, 1982a: Severe weather occurring in areas of low surface dew points. *Preprints 12th Conf. Severe Local Storms,* San Antonio, Amer. Meteor. Soc., 143–146.

——, 1982b: A synoptic climatology of northwest flow severe weather outbreaks. Part I: Nature and significance. *Mon. Wea. Rev.,* **110,** 1653–1663.

——, and W. D. Hirt, 1983: The derecho . . . a severe weather producing convective system. *Preprints 13th Conf. Severe Local Storms,* Tulsa, Amer. Meteor. Soc., 178–181.

Kelly, D. L., J. T. Schaefer, R. P. McNulty, C. A. Doswell III and R. F. Abbey, Jr., 1978: An augmented tornado climatology. *Mon. Wea. Rev.,* **106,** 1172–1183.

Maddox, R. A., 1980: Mesoscale convective complexes. *Bull. Amer. Meteor. Soc.,* **61,** 1374–1387.

——, and C. A. Doswell III, 1982: An examination of jetstream configurations, 500 mb vorticity advection and low-level thermal advection patterns during extended periods of intense convection. *Mon. Wea. Rev.,* **110,** 184–197.

Marwitz, J. D., 1972a: The structure and motion of severe hailstorms. Part I: Supercell storms. *J. Appl. Meteor.,* **11,** 166–179.

——, 1972b: The structure and motion of severe hailstorms. Part II: Multi-cell storms. *J. Appl. Meteor.,* **11,** 180–188.

——, 1972c: The structure and motion of severe hailstorms. Part III: Severely sheared storms. *J. Appl. Meteor.,* **11,** 189–201.

McNulty, R. P., 1978: On upper tropospheric kinematics and severe weather occurrence. *Mon. Wea. Rev.,* **106,** 662–672.

Miller, R. C., 1972: Notes on analysis and severe storm forecasting procedures of the Air Force Global Weather Central. Tech. Rep. 200 (Rev.), Air Weather Service, 190 pp. [Available from Scott AFB, IL 62225.]

Newton, C. W., 1950: Structure and mechanism of the prefrontal squall line. *J. Meteor.,* **7,** 210–222.

——, 1963: Dynamics of Severe Convective Storms. *Severe Local Storms. Meteor. Monogr.,* No. 27, Amer. Meteor. Soc., 33–58.

——, and S. Katz, 1958: Movement of large convective rainstorms in relation to winds aloft. *Bull. Amer. Meteor. Soc.,* **39,** 129–136.

——, and H. R. Newton, 1959: Dynamical interactions between large convective clouds and environment with vertical shear. *J. Meteor.,* **16,** 483–496.

Notis, C., and J. L. Stanford, 1973: The contrasting synoptic and physical character of northeast and southeast advancing tornadoes in Iowa. *J. Appl. Meteor.,* **12,** 1163–1173.

——, and ——, 1976: The synoptic and physical character of Oklahoma tornadoes. *Mon. Wea. Rev.,* **104,** 397–406.

Palmén, E., and C. W. Newton, 1969: *Atmospheric Circulation Systems.* Academic Press, 344–350.

Purdom, J. F. W., 1976: Some uses of high-resolution GOES imagery in the mesoscale forecasting of convection and its behavior. *Mon. Wea. Rev.,* **104,** 1474–1483.

Reed, R. J., 1979: Cyclogenesis in polar air streams. *Mon. Wea. Rev.,* **107,** 38–52.

Sangster, W. E., 1958: An investigation of nighttime thunderstorms in the central United States. Tech. Rep. No. 5, Contract AF 19(604)-2179, University of Chicago, 32 pp. [Available from Sci. Ser. Div., Central Region Office, Room 1747, NWS, 601 E. 12th St., Kansas City, MO 64106.]

Schaefer, J. T., and C. A. Doswell III, 1979: On the interpolation of a vector field. *Mon. Wea. Rev.,* **107,** 458–476.

Showalter, A. K., 1953: A stability index for thunderstorm forecasting. *Bull. Amer. Meteor. Soc.,* **34,** 250–252.

Uccellini, L. W., and D. R. Johnson, 1979: The coupling of upper and lower tropospheric jet streaks and implications for the development of severe convective storms. *Mon. Wea. Rev.,* **107,** 682–703.

Williams, R. J., 1976: Surface parameters associated with tornadoes. *Mon. Wea. Rev.,* **104,** 540–545.